

# Physical Properties and Behaviour of High-Performance Concrete at High Temperatures

---

U. SCHNEIDER, M. C. ALONSO, P. PIMIENTA and R. JANSSON

## ABSTRACT

The following report gives an overview of the TC program and some preliminary results.

## 1. INTRODUCTION

The Technical Committee TC 227 HPB was established by the RILEM Council in 2007. The first committee meeting took place in Coimbra, Portugal in November 2007. The program of the new TC was prepared by members of the former TC 200 HTC “Mechanical Concrete Properties—Modelling and Applications”.

The objectives of the new TC comprise the characteristic behaviour, physical properties and modelling of different types of high performance concrete (HPC) at temperatures of up to 1000°C including the effects of the exposure of concrete structures to fire. The behaviour of five types of HPC is under the main focus of the TC (see fig. 1). Among these are high strength concrete (HSC), ultra high performance concrete (UHPC), self compacting concrete (SCC), special temperature resistant concrete (STRC) and special aggregate concrete (SAC), please see fig. 1. The topic of high strength concrete is of major interest for the TC.

The TC HPB started its work program with 18 members and now has 28 members. The increase in membership shows the great international interest in the field of HPB research and application.

---

U. Schneider, Vienna University of Technology, Karlsplatz 13, 1040 Vienna, Austria

M. C. Alonso, IETcc, Serrano Galvanche 4, 28033 Madrid, Spain

P. Pimienta, CSTB, Departement Securite, Structures et Feu, 84, avenue Jean Jaures, F-77447 Marne la Vallee, Cedex 02, France

R. Jansson, SP Technical Research Institute of Sweden, Fire Technology—Fire Resistance, Brinellgatan 4, Box 857, SE-501 15 Boras, Sweden

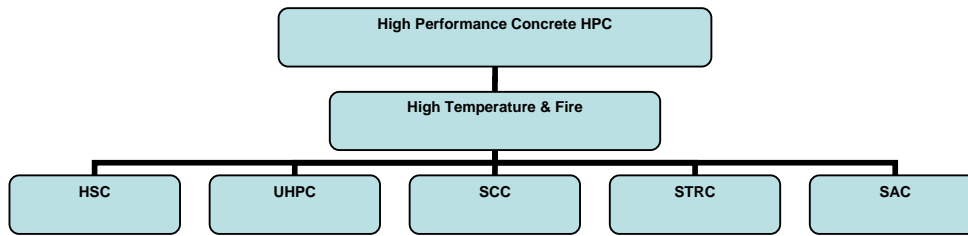


Figure 1. Concretes investigated within the work program of the proposed TC.

## 2. PROGRAM AND WORK GROUPS

The work program of the TC is divided into the following tasks:

Task 1: State of Art Report on HPC Properties

Task 2: Technical Report on Spalling of HPC

Task 3: Technical Report on Pore Pressure Measurements

Task 4: State of Art Report on Modelling

Task 5: Experimental Methods and Data

Sub-Task 5.1: Fracture Energy Methods

Sub-Task 5.2: Thermal Property Methods

Sub-Task 5.3: Permeability Methods and Properties

Sub-Task 5.4: Temperature Measurements

Sub-Task 5.5: Weight Loss Measurements

For the different task programs individual Work Groups (WG) have been set up. Now there are six work groups which work in the areas 1 to 4, 5.1 and 5.3.

## 3. STAR ON PROPERTIES AND BEHAVIOR OF HIGH-PERFORMANCE CONCRETE

### 3.1 Introduction

### 3.2 Degradation reactions in HPB at high temperatures in relation with conventional concrete

When portland cement concrete is subjected to heat, a number of transformations and reactions of different kinds occurs even at a moderate rise in temperatures. These phenomena comprise the so-called degradation reactions, which bring about a progressive breakdown in the micro structure of the concrete. They occur particularly in the hardened cement paste, but may also occur in the aggregate. The thermal analyses clearly reveal the reactions in cement paste, caused by temperature effects like a) water expulsion at about 100°C; b) breakdown of CSH gel (first stage of dehydration) at 180°C; c) decomposition of portlandite at 500°C; d) transformation of quartz at 570°C; e) decarbonation of limestone from 800°C onwards; f) start of melting from 1150 C–1200°C onwards, as figure 2 left shows.

The structure of CSH gel initiates alterations at temperatures above 100°C, as shown in figure 2 right. The initial CSH structure is considered to be formed by chains of silica-tetrahedrate, indicated by peak of ( $Q^1$ ) in figure, associated to tetrahedrate at the extreme of the chain and by ( $Q^2$ ) tetrahedrate in the middle of the chain. The binding water is located in between the CSH chains. This water is progressively lost during heating as water vapor, that constitutes the well

identified dehydration processes of CSH cement paste, by thermal analysis as indicated in figure 1 (left), and further to the built up of pore pressures.

However the chain structure of the CSH also suffers transformation due to heating, which can be identified with  $^{29}\text{Si}$  MAS-NMR, as shows figure 2 (right). After temperatures above  $200^\circ\text{C}$  the ( $Q^1/Q^2$ ) ratio increases indicating that silicon chains initiate breaking and at  $400^\circ\text{C}$  the CSH structure has been completely destroyed. Simultaneously to these transformations in CSH, a new nesosilicate phase of monomers of silicon tetrahedrate is formed ( $Q^0$ ) having a similar but less crystalline structure than the anhydrous cement grains of larnite. The CSH degradation with temperature contributes to mechanical strength losses.

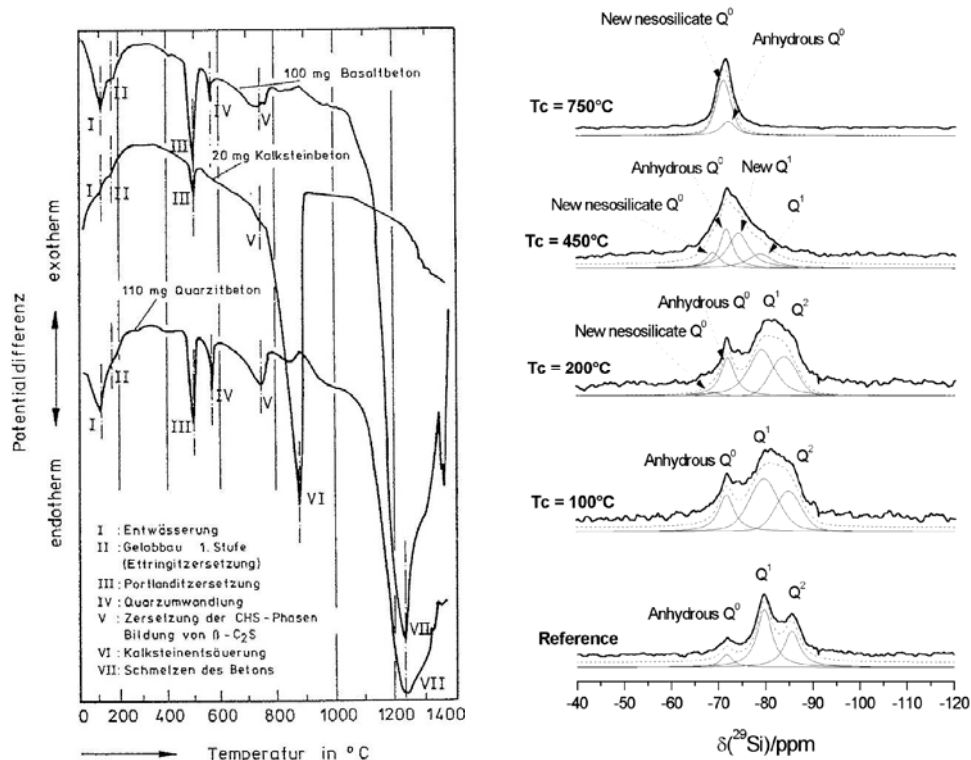


Figure 2. Left- Differential thermal analysis of various normal weight concretes, Right- CSH transformations with temperature as shown with  $^{29}\text{Si}$  MAS-NMR spectra (C. Alonso).

In the case of High Performance Concretes (HPC) or Self Compacting Concrete (SCC), the thermograms follow a similar evolution with temperature, as figure 3 shows. The changes in portlandite  $\text{Ca}(\text{OH})_2$  also takes place at similar temperatures. Although the thermal transformation of this component occurs abruptly but not a progressive dehydration as follows the CSH transformations with increasing temperature. The high contents of mineral additions, many times employed in the production of HPC, diminishes or even eliminates completely the region of transformation of portlandite at  $450^\circ\text{C}$  due to its lower content, that certainly changes the processes occurring at high temperature in the cement paste.

Other differences are in the type of aggregate used, usually of smaller size, figure 2 (left). If gabbro and quartzite are used, do no suffer mass loss but the use of lime as aggregate decomposition occurs above  $750^\circ\text{C}$ , however the clear difference in the amount of mass loss is detected in SCC due to lime transformation coming from not only the aggregate but also from the calcareous

filler, typically employed for production of SCC, figure 2 (right). At 1200°C all the concrete components have dehydrated completely and melting initiates, similarly to conventional concrete. In fact in conventional concrete, the liquefaction of the concrete commences with the melting of the matrix of hardened cement paste that begins to melt at about 1200° C and that melting of the aggregates takes place only after this.

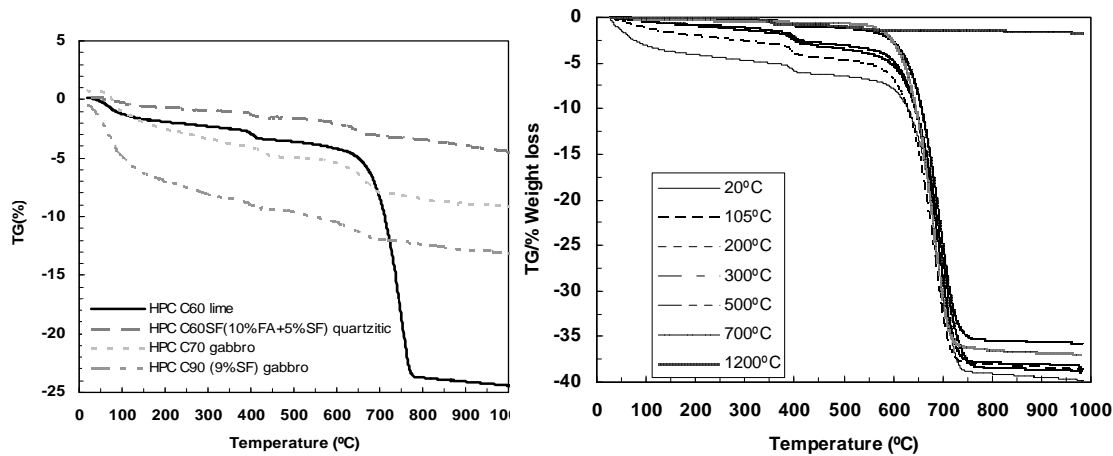


Figure 3. Differential thermal analysis of various concretes. Left: TG for HPC and Right: TG for SCC (C. Alonso, L. Fernandez)

### 3.3 Mechanical properties of concrete at high temperatures

In this field a PhD thesis has been submitted by S. Huismann (G) at the Vienna University of Technology. Parts of the thesis are presented in this conference.

## 4. REPORT ON SPALLING OF HPC

### 4.1 Introduction

The Work Group 2 for Spalling has made great progress in the past two years and an international workshop was organized by TC members F. Dehn and E. Koenders in Germany in 2009. In total, the workshop has written 51 reports on 548 pages. The following provides a short introduction into spalling of HCP under ISO fire conditions and in microwave tests.

### 4.2 Test method and results for spalling

The spalling of concrete during heating up is well known since several decades. Generally it is assumed that spalling is caused by the thermo-hydraulic effects due to vaporization of capillary and gel water, by the chemical phase changes during heating and by the thermo-physical effects due to thermal stresses. Those effects may occur in the hardened cement paste (HCP) and as well in aggregates used in concrete. From fire tests it is known that the spalling of concrete is mainly caused by vapor pressure in capillary and gel pores being filled with residual parts of mixing water after the hydration. Up to now the connection between pore pressure and spalling of concrete is not clear. It is neither known how the chemical water in concrete influences the spalling effect. From HPC and UHPC it is known that those types of concrete may explode

heavily under fire attack, respectively, even if they do not contain nearly any capillary water and are generally produced at very low water/cement ratios.

In the following a few preliminary results concerning investigations with respects to principal parameters influencing spalling of concretes are given. The reference concrete is an ordinary concrete (B40), which has been used for the construction of a tunnel in France. B60 concrete has been fabricated by only varying the W/C ratio (by increasing cement content and reducing water content) and by fixing the aggregates quantity constant. Exactly the same material has been used to fabricate the 2 concretes. The compressive strength of B60 is higher than 60 MPa. This concrete is considered an HPC.

Figure 4 presents pictures taken on several slabs after ISO fire tests and moderate heating rate. After the tests the volume of spalled concrete layers was determined by mapping. Thanks to these mappings, maximal depth and volume of concrete that had been ejected during heating were assessed.

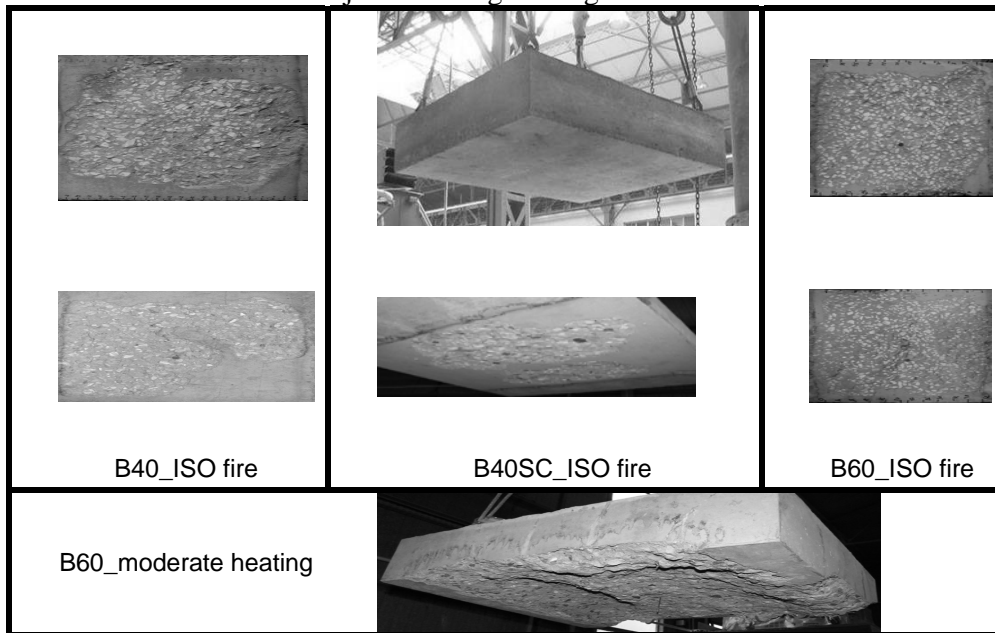


Figure 4.1. Views of the exposed surface of slabs after one hour of ISO fire (spalling between the 10th and the 20th minute of the test accord. to Pimienta).

From the mapping results, the following observations were obtained:

The dense concrete (HPC) ejected more concrete and larger damage (i.e. deeper and greater damaged zone),

Only one of the B40SC slabs showed little surface spalling. The spalling induced damage for this slab is weak like similar concretes which are fabricated only with calcareous aggregates.

The result underlines the important influence of aggregate type on the risk level of concrete thermal instability and its characteristics,

During moderate heating (i.e. for very slower heating than ISO fire) on B40 slabs, no spalling was observed whereas spalling of B60 has been observed in that case. Under ISO fire conditions the B60 lost a 6 cm thick concrete layer by spalling.

From these measurements it appears that no clear link exists between the built-up of vapour pressure and concrete spalling potential. This result is not in accordance with classical interpretations that state that concrete spalling is dependent on the vapour pressure level. We also note that this pressure level is

very low compared to concrete tensile strength. Some special test configurations (slow heating on cylindrical sample and moderate heating on slabs) led to high vapour pressures but without any concrete spalling. Based on these results it is assumed that vapour pressure is not the only physical origin for concrete spalling.

Contrary to these results microwave experiments show that spalling is mainly caused by the input of thermal energy, i.e. local increase of pressure in the pore system of the specimen so that the explosive spalling is a common appearance regardless of the type of cement, w/c-ratio, curing and test age etc. The reason of the local spalling is a result of structural defects of the specimen which appear in the specimen during the compacting and hydration (build-up of nano (gel) pores), but it cannot be excluded that local shrinkage cracks or differences in strength occur (see fig. 4.2 and 4.3 according to Schneider).



Figure 4.2. Explosive Spalling of HPC-Paste.

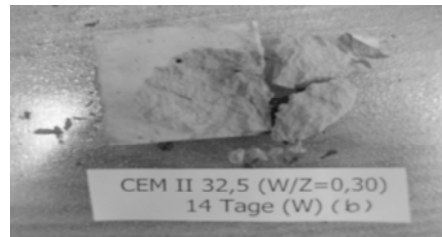


Figure 4.3. Local Spalling of HPC-Paste.

The spalling of specimen occurred mainly after 2-3 minutes of MW-heating. The observed temperatures of spalling range from 100 °C to 250 °C. The larger specimen and specimen with higher strength or longer curing time needed more energy until spalling. The mass specific energy absorption was determined ranging from 300 J/g to 600 J/g for all specimen of the 86 series tested.

## 5. WG 3 PORE PRESSURE MEASUREMENT

Measurement of the pore pressure in concrete can be done with either embedded or external measurement gauges. Embedded gauges means that the measurement is performed in the high temperature zone. With external gauges the pressure is transferred from the measurement point to a gauge outside the specimen by a pipe from inside the specimen. When measuring the pressure development in concrete the corresponding temperature is important. In some systems the temperature is measured in the pressure measurement devices and in some experimental setups the temperature is measured externally. The most common different pressure measurement setups shown in figure 5.1 include:

- A. Embedded pipe, which transforms the pressure to an external pressure gauge. In this and other similar applications (B-D) the pipe exits the specimen away from the heat source (Jansson).
- B. Embedded pipe with internal rod, which transforms the pressure to an external pressure gauge. The internal rod is used to reduce the volume in the pipe. A cavity is created around the measurement point (Schneider).
- C. Embedded pipe with clamped sintered material in contact with the concrete, which transforms the pressure to an external pressure gauge. A thermocouple is included in this method to monitor temperature. The thermocouple can be introduced either as a volume reducer in the pipe (Kalifa) as shown in Figure 1, or externally to the pipe (Phari).

- D. Embedded pressure gauge (Consolazio).
- E. Embedded pipe, which transforms the pressure to an external pressure gauge. In this application the pipe parallel to the heated surface.

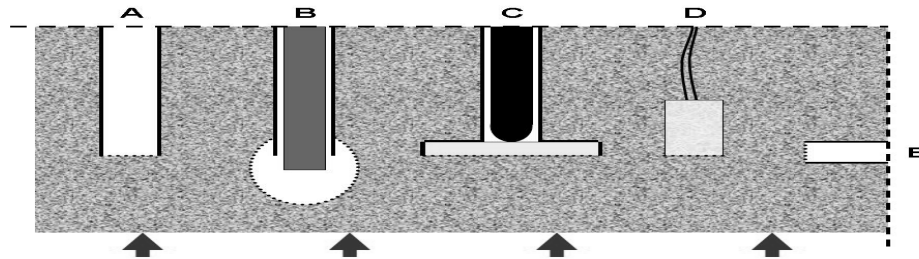


Figure 5.1. Different pressure measurement setups according to Jansson. Heating heated from below.

In measurement setup types A, B, C, D and E the pressure is transformed to the outside of the concrete using a medium in the pipe. In different applications of these methods the following media have been used: a) air, b) water, c) oil, d) mercury.

A direct comparison of the results from different methods is not possible. Therefore some general potential sources of error may be discussed. Cracks around the sensor which could lead to depressurisation of the measurement point are of major concern. All systems could potentially suffer from this problem to a lesser or greater degree. Ultimately a type D setup with a very small pressure gauge and the electrical wires exiting the specimen along the isotherms (horizontally in figure 1) would be preferable. The type E setup with a pipe exiting along the isotherms is promising but if this system contains oil a careful analysis of the influence of oil expansion must be made. Similar analysis for an oil filled pipe exiting away from the hot zone, i.e. type A, shows that oil expansion during rapid heating in this configuration is not a problem. In the case of a Type C arrangement a possible error might be that compared with the surrounding concrete an extra portion of liquid moisture might be trapped in the sintered material giving rise to a potential error. Despite the above mentioned potential errors, pressure measurement studies to date have shown that:

The pore pressure development in heated high strength concrete is higher than in normal concrete (Schneider, Kalifa, Phan, Mindeguia).

Higher initial moisture content leads to higher pore pressure (Phan).

Slow heating generally leads to higher pressure than faster heating (standard fire), probably due to induced thermal damage during fast heating (Mindeguia, Phan).

An addition of polypropylene fibre reduces the pressure in concrete that does not spall (Schneider, Phan, Mindeguia).

The direct connection between fire spalling and pore pressure is weak during fire exposure of large externally loaded specimens, i.e. concrete with the addition of polypropylene fibres that does not spall typically exhibits higher pressure than a concrete without polypropylene fibres that spalls (Jansson, Boström, Consolazio).

## 6. STAR ON MODELLING

### 6.1 Introduction

### 6.2 Chapters and writers

More than ten TC members are involved in the work of modelling. Several parts of the chapters have been drafted and a few of the writers participate in this conference. Therefore no specific details of preliminary results are presented in this report. Further information may be obtained from the chairman of the Work Group 4, A. Millard, CEA, France and F. Pesavento, Univ. of Padova, Italy.

## 7. FRACTURE PROPERTIES OF HPC AT HIGH TEMPERATURES

### 7.1 Introduction

### 7.2. Test methods and results

Within the WG 5.1 a new test method for  $K_{I,E}$  and  $K_{II,C}$  and  $G_f$  measurements at high temperatures has been developed. A joint research program in which OPC and HPC specimens were tested at temperatures up to 700°C has been carried out at the Belarus State University of Technology and at the Vienna University of Technology. The tests were carried out by means of concrete cubes 5 or 10 cm in length. Fig. 7.1 and 7.2 show the test set-up for this type of fracture tests with cubes at high temperatures.

Figure 7.1. Fracture test method for  $K_{IC}$  values of HPC (Schneider).

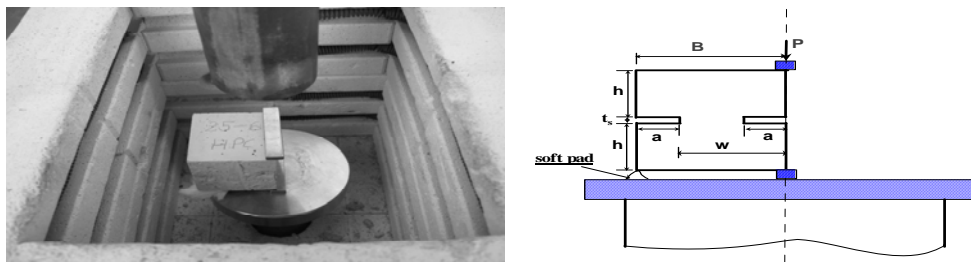
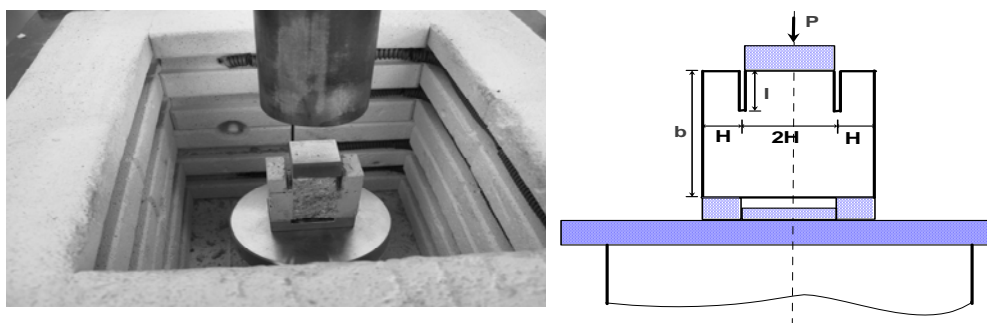


Figure 7.2. Fracture test method for  $K_{IIC}$  values of HPC (Schneider).





The latest test results for  $K_{IC}$  and  $K_{IIC}$  which were derived from 10 cm cube tests of HPC with a strength of 86 N/mm<sup>2</sup> and after 28 days of curing are given in table 7.1.

Table 7.1. Results of measures  $K_{IC}$  and  $K_{IIC}$  values and concrete strength at high temperatures according to Leonovich (Minsk).

Temperature (°C)	$f_{c,28}$ (MPa)		$K_{IC}$ (MN/m <sup>3/2</sup> )		$K_{IIC}$ (MN/m <sup>3/2</sup> )	
	I	II	I	II	I	II
20	85,7	87,5	0,89	0,82	5,82	4,62
100	83,6	-	0,88	0,85	4,45	5,03
200	83,6	-	0,88	1,00	3,45	6,32
300	99,5	100,4	0,72	0,83	3,61	5,90
400	102,2	110,6	0,35	0,76	3,33	4,77
500	88,7	92,1	0,32	0,37	2,09	3,76
600	81,0	-	0,27	0,24	1,25	3,43
700	76,3	-	0,26	0,19	1,46	1,20

Similar results were obtained for  $K_{IC}$ -values derived from 5 cm cubes with a strength of 84 N/mm<sup>2</sup> after curing. The test results are given in fig. 7.3. Each test value is the average of at least 3 measurements. The values of  $K_{IC}$  for specimen after 90 days of curing at 300°C are unexpectedly low compared to the 120 day data. In principal the measurements are in agreement with the data given in table 7.1.

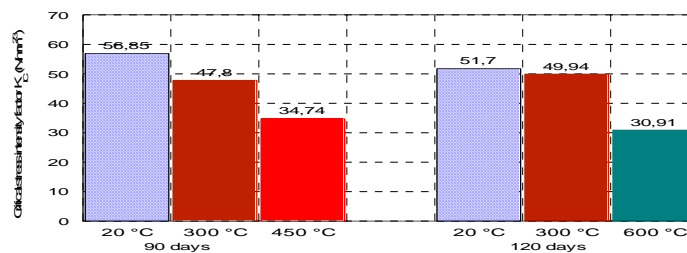


Figure 7.3.  $K_{IC}$ -values of HPC after 90 and 120 days of curing according to Schneider.

## 8. STAR ON PERMEABILITY OF HPC AT HIGH TEMPERATURES

There are two TC members working in the field of permeability measurement: G. Debicki, INSA Lyon (France) and U. Schneider, Vienna University of Technology (Austria). The theoretical background has recently been completed and two test methods for measurements have in the meantime been developed. As part of the conference new test results will be presented in a separate paper by the Vienna University of Technology.

## 9. FINAL REMARKS

The TC 227 HPB has a life-span of 5 to 6 years and reaches its first period of 3 years in September 2010. It is very likely that several STARs and reports will be finalized during the second period and we look forward to getting inputs from experts from all over the world.